

Local- and Intermediate-Range Atomic Structures of $(\text{Ga}_2\text{S}_3)_{0.25}(\text{GeS}_2)_{0.75}$ Glass: Complementary Use of X-Rays and Neutrons

Shinya HOSOKAWA^{1,2}, Yohei ONODERA³, László PUSZTAI^{4,5}, Jens Rüdiger STELLHORN⁶, Hiroo TAJIRI⁷, Kazutaka IKEDA⁸, and Toshiya OTOMO⁹

¹Faculty of Materials for Energy, Shimane University, Matsue 690-8504, Japan

²Institute of Industrial Nanomaterials, Kumamoto University, Kumamoto 860-8555, Japan

³Center for Basic Research on Materials, National Institute for Materials Science (NIMS), Tsukuba 305-0047, Japan

⁴HUN-REN Wigner Centre for Physics, H-1525 Budapest, Hungary

⁵International Research Organization for Advanced Science and Technology (IROAST), Kumamoto University, Kumamoto 860-8555, Japan

⁶Co-Creation Institute for Advanced Materials, Shimane University, Matsue, 690-8504, Japan

⁷Japan Synchrotron Radiation Research Institute (JASRI), Sayo 679-5198, Japan

⁸Neutron Industrial Application Promotion Center, Comprehensive Research Organization for Science and Society (CROSS), Tokai 319-1106, Japan

⁹High Energy Accelerator Research Organization (KEK), Tsukuba 305-0801, Japan

E-mail: s_hosokawa@mat.shimane-u.ac.jp

(Received December 23, 2024)

Local- and intermediate-range atomic arrangements in a $(\text{Ga}_2\text{S}_3)_{0.25}(\text{GeS}_2)_{0.75}$ glass, having a high infrared transparent coefficient, were investigated by a combination of anomalous X-ray scattering (AXS), X-ray and neutron diffraction (XRD and ND), and reverse Monte Carlo (RMC) modeling, which are compared with our previous results of a similar $(\text{Ga}_2\text{Se}_3)_{0.25}(\text{GeSe}_2)_{0.75}$ glass (JPS Conf. Proc. **33**, 011069 (2021)). By adding the ND structure factor and pair distribution function to AXS and XRD results, reasonable partial structure factors and partial pair distribution functions were obtained, even applying no constraints of shortest interatomic distances during the RMC calculation procedure. Total coordination numbers around Ga, Ge, and S atoms are 3.55, 3.88, and 2.77, respectively, which contradict the 8 – *N* rule except around Ge. The numbers of Ga-Ga, Ga-Ge, Ge-Ga, Ge-Ge, and S-S wrong bonds were found to be 0.34, 0.54, 0.36, 0.63, and 1.21, respectively. Small but clear differences are found by comparing with the results of selenide glass. In the three-dimensional atomic configuration, the structure looks inhomogeneous in both density and concentration as in the selenide glass.

KEYWORDS: Neutron diffraction, Anomalous X-ray scattering, Reverse Monte Carlo modeling, Glass structure

1. Introduction

Chalcogenide glasses are characterized by remarkable physical properties [1], such as high infrared transparency [2] and large photosensitivity [3]. In general, their properties can be fine-tuned by varying the composition of the constituent elements. An excellent example is a Ga-Ge-chalcogenide alloy having a high infrared transparency, which can be used for infrared telecommunications as a glass-fiber material. Although accurate structural characterization of these glasses is very important to link to the unique properties, experimental works are still heavy tasks. In case of the Ga-Ge-Se

alloys, the constituent elements of Ga, Ge, and Se in these glasses have similar atomic numbers, corresponding to similar atomic form factors for X-ray diffraction (XRD), f . For X-ray absorption fine structure (XAFS) spectroscopy, they have similar backscattering amplitudes, and it is very difficult to discriminate the elements of neighboring atoms by the XAFS measurements. Moreover, the scattering lengths for neutron diffraction (ND), b , also have only small differences from each other, i.e., 7.288, 8.185, and 7.970 fm for Ga, Ge, and Se atoms [4], respectively, and it is hard to obtain the spectral contrasts between the XRD and ND data.

In the case of the Ga-Ge-S alloys, the atomic number of S is much smaller than that of Se; however, it does not help the structural investigation of these alloys. The b_S for ND is a small value of 2.847 fm [4] as well as the small f_S value for XRD. The S K absorption edge is located in the soft X-ray region of 2.472 keV, which makes the XAFS or anomalous X-ray scattering (AXS) experiments to be very tough works.

The existence of metal-metalloid (Ga-Ge) bonds in the Ga-Ge-Se alloys was confirmed by Raman and NMR data [5], and ND and XAFS measurements combined with reverse Monte Carlo (RMC) modeling [6]. The nature of such ‘wrong’ bonds is, however, still largely disputed, i.e., some studies claimed only Ge-Ge homopolar bonds [5] while others found only Ga-Ge bonds [6]. Klee et al. carried out anomalous X-ray scattering (AXS) [7] and applied that several constraints of dismissing pairs of Ga and Ge in the RMC modeling. However, no specific pairs could be found for the constraints of the RMC fits. Recently, Hosokawa et al. reported the results of AXS, XRD, and ND in combination with RMC modeling on a $(\text{Ga}_2\text{Se}_3)_{0.25}(\text{GeSe}_2)_{0.75}$ (GaGeSe) glass [8]. They found the meaningful existences of ‘wrong bonds’ in all the pairs of Ga and Ge atoms.

Subsequent to this study, we have carried out a similar structural study on a $(\text{Ga}_2\text{S}_3)_{0.25}(\text{GeS}_2)_{0.75}$ (GaGeS) glass by AXS close to the Ga and Ge K absorption edges, XRD, and ND, in combination with the RMC analysis. We will discuss the similarities and differences between these Ga-Ge-chalcogenide glasses.

2. Experimental and data analysis procedure

A mixture of pure elements with the concentration of GaGeS was sealed in a quartz ampoule, which was heated using a furnace to 1050°C and kept for 12 h. The temperature was reduced to 850°C by 2°C/min, and kept for 1 h, followed by a quench in cold water. Then, the sample was annealed at 350°C for 3 h, and gradually cooled down to room temperature.

The AXS experiments were carried out at the beamline BL13XU of the SPring-8 [9]. The principle and experimental procedure of AXS were given elsewhere [10–12]. Two scattering experiments were performed to obtain differential structure factors, $\Delta_k S(Q)$, at 20 and 200 eV below the Ga (10.367 keV) and Ge (11.104 keV) K edges. For the analysis, theoretical values of the real and imaginary parts of the anomalous terms of the atomic form factor calculated by Sasaki [13] were used. The energy-independent theoretical atomic form factors [14] were also used for obtaining $\Delta_k S(Q)$. The total XRD structure factors, $S_X(Q)$, were obtained at the incident X-ray energy of 10.904 keV.

The ND experiments were performed to obtain total ND structure factors, $S_N(Q)$, in a wide Q range from 1.6 to more than 1000 nm⁻¹ using the NOVA spectrometer [15] installed at BL21 of the Material and Life Experimental Facility (MLF) of the Japan Proton Accelerator Research Complex (J-PARC), Tokai, Japan. The sample was contained in a V-Ni null scattering sample container with an outer diameter of 6.0 mm and a thickness of 0.1 mm. The incident neutron beam was generated by the proton accelerator with an output power of 700 MW, and the ND experiment took about 3 h. Measurements were performed in the time-of-flight mode, with neutron energies between 0.0013 and 5.7 eV, and a pulse repetition rate of 25 Hz. Details of the neutron detecting procedures are given elsewhere [16]. The observed scattering intensities from the sample were corrected for instrumental background, absorption of the sample and the cell [17], multiple [18], and incoherent scattering.

Table I. W_{ij}^k for the i - j correlations by k scattering methods.

$k \backslash i-j$	Ga-Ga	Ga-Ge	Ga-S	Ge-Ge	Ge-S	S-S
$\Delta_{\text{Ga}}S(Q)$	0.1737	0.3207	0.4247	0.0362	0.0487	-0.0040
$\Delta_{\text{Ge}}S(Q)$	-0.0194	0.2143	-0.0449	0.3296	0.5235	-0.0031
$S_X(Q)$	0.0475	0.1348	0.2039	0.0973	0.2942	0.2223
$S_N(Q)$	0.0508	0.1707	0.1784	0.1435	0.2999	0.1567

The scattering lengths and absorption cross-sections for the constituent nuclei were taken from the literature [4]. These corrections were performed by the nvaSq program package coded by the NOVA group [19].

Table I shows the weighting factors W_{ij}^k for the i - j correlations by k scattering methods ($\Delta_{\text{Ga}}S(Q)$, $\Delta_{\text{Ge}}S(Q)$, $S_X(Q)$, and $S_N(Q)$) for the partial structure factors, $S_{ij}(Q)$. Note that these values are given at $Q = 23 \text{ nm}^{-1}$ near the first peak positions, and the W_{ij}^k values slightly vary with Q for three X-ray scattering methods. As seen in the table, if i or j corresponds to k , W_{ij}^k is enhanced, while if this is not the case, W_{ij}^k is highly suppressed. Another striking feature in this table is that W_{ij}^k for $S_X(Q)$ and $S_N(Q)$ have very small differences from each other, with which it is difficult to obtain partial structures from only the contrast between the XRD and ND data.

The present RMC calculation was carried out by using the RMC++ program package [20]. Initial configurations were generated by hard-sphere Monte Carlo simulation. The simulation box contained totally 10,000 atoms in a size of 6.377 nm, which was chosen to adjust the number density of the sample, 38.57 nm^{-3} . From the RMC fits, $S_{ij}(Q)$, partial pair distribution functions $g_{ij}(r)$, and the corresponding 3D atomic configurations were obtained.

3. Results

Circles in Fig. 1(a) show, from top to bottom, experimental data of $\Delta_{\text{Ga}}S(Q)$ and $\Delta_{\text{Ge}}S(Q)$ taken from AXS, $S_X(Q)$, and $S_N(Q)$. The solid curves represent the corresponding RMC fits. Here, we explain the naming rule for peaks in $S(Q)$ spectra in the glass field. The peaks located usually at about 10, 22, and 35 nm^{-1} are called the first sharp diffraction peak (FSDP) or prepeak, first or primary peak, and second peak, respectively, because FSDP is not observed in usual non-crystalline or liquid materials such as metallic ones. As seen in the figure, the spectral features are very different from each other, owing to different W_{ij}^k s for $S_{ij}(Q)$ s as shown in Table I. In particular, the heights of the FSDPs located at about $Q = 10 \text{ nm}^{-1}$ are different from each other. Note that the FSDP heights are much larger than those of GaGeSe glass given in Fig. 1(a) of Ref. [8]. At the first peak position of about $Q = 21 \text{ nm}^{-1}$, the RMC fit does not reproduce the experimental $\Delta_{\text{Ge}}S(Q)$ result, where a minimum is seen. We speculate that this is due to the lack of $\Delta_{\text{S}}S(Q)$ data with a large maximum compensating the minimum in $\Delta_{\text{Ge}}S(Q)$ at the same Q position, as observed in the GaGeSe glass. Another discrepancy is that the spectral features in $\Delta_{\text{Ga}}S(Q)$ are similar to those in $\Delta_{\text{Ge}}S(Q)$ for the GaGeS glass. Thus would be owing to the fact that the atomic arrangements around Ga resemble those around Ge in the GaGeS glass rather than those in the GaGeSe glass.

Figure 1(b) shows the experimental and analytical results for $g_N(r)$, which has a sharp and well-defined first peak at about 0.22 nm and a second peak at about 0.34 nm. The coincide between the experiments and fits are quite good. The above lengths are smaller than those of the GaGeSe glass [8], which may be due to the shorter atomic bond lengths around S than those around Se.

Figure 2(a) shows $S_{ij}(Q)$ s obtained from the RMC fits. The features of $S_{ij}(Q)$ s highly depend on the combinations of partial elements. In the combinations of the Ga and Ge elements, large and sharp peaks with a height of about 3 are observed at the FSDP positions of the total $S(Q)$ s of about $Q = 10$

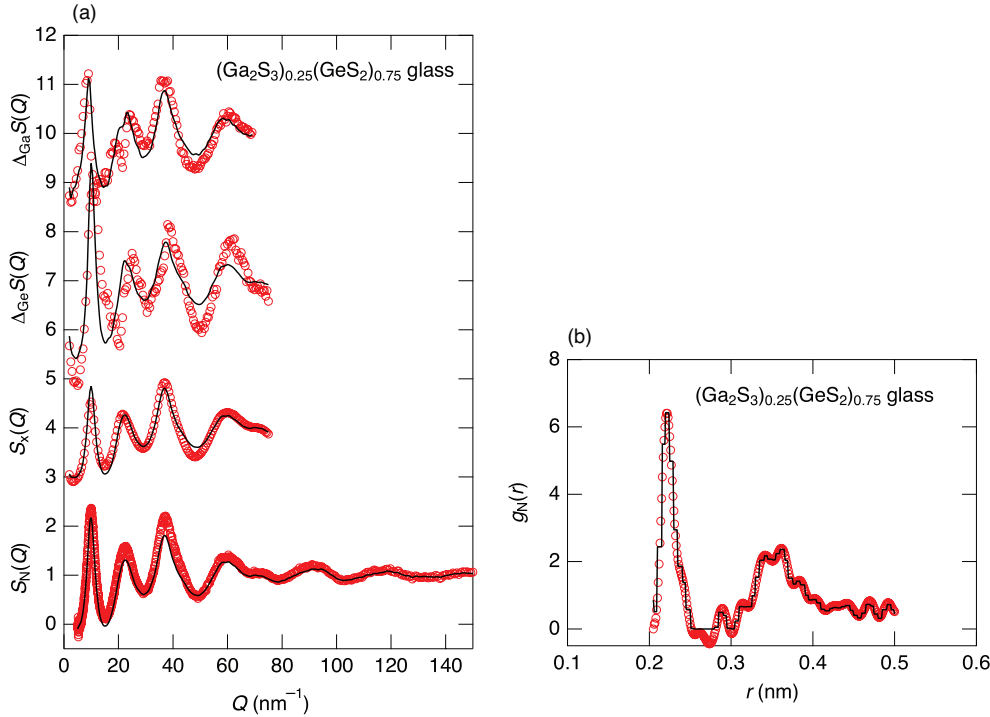


Fig. 1. (a) From top to bottom, circles show experimental data of $\Delta_{\text{GaS}}(Q)$ and $\Delta_{\text{GeS}}(Q)$ taken from AXS, $S_X(Q)$, and $S_N(Q)$, and the solid curves represent the RMC fits. (b) The same meaning for $g_N(r)$.

nm^{-1} , which are similar to those of GaGeSe glass. A difference is found in the large FSDP in the Ge-S partial with a height of about 2, while a small peak with a height of only 0.3 was detected in the Ge-Se partial of the GaGeSe glass [8]. Besides, the other S-related partials have small FSDP signals. At the first peak position of about $Q = 21 \text{ nm}^{-1}$, the S-related correlations show small peaks, while the others exhibit middle-sized peaks. These results are not similar to those in the GaGeSe glass, where large, middle, and small peaks are observed in the Se-Se, Ga-Se, and Ga-Ga correlations, respectively, whereas the Ga-Ge, Ge-Ge, and Ge-Se partials have ‘negative’ pits at this Q [8].

Figure 2(b) shows $g_{ij}(r)$ s obtained from the RMC fits. The first peaks of most partials show similar features with the height of more than 6, while that of S-S represents a small peak with the height of about 3. These spectral features are very different from those of GaGeSe glass showing a variety of heights [8]. It is interesting that the present GaGeS glass has small numbers of cation homopolar ‘wrong’ bonds although they were also found with large magnitudes in the GaGeSe glass. The second peaks at about 0.36 nm exhibit interesting features; 1) the cation-S correlations show small peaks at the longer positions indicating that the cation-(S)-S correlations are small, 2) the cation-cation correlations show large peaks with relatively shorter positions corresponding to the cation-S-cation correlations, and 3) the S-S partial exhibits small and broad peak being composed of the mixture of S-Ga-S and S-Ge-S connections.

4. Discussion

To analyze the local atomic structures of this GaGeS glass in detail, partial interatomic distances between the i - j pairs, r_{ij} are listed in Table II. All of the r_{ij} values are mostly the same values of 0.218-0.225 nm for either heteropolar or homopolar bonds, although the Ga-related ones are slightly longer. Pethes et al. reported the partial structures of the same GaGeS glass by measuring total XRD

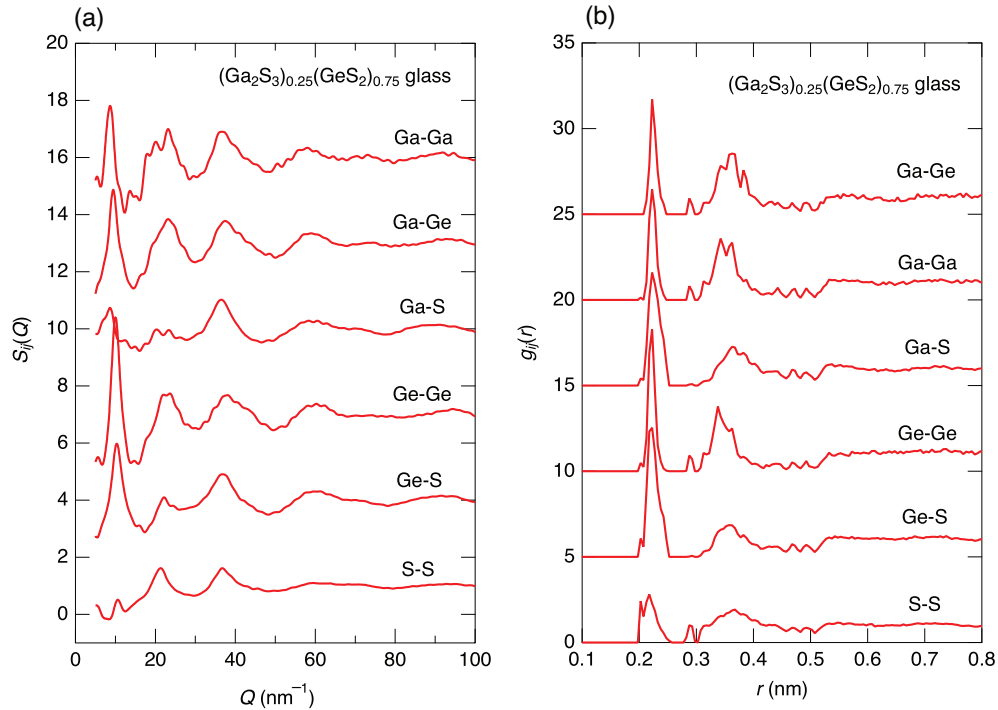


Fig. 2. (a) $S_{ij}(Q)$ s and (b) $g_{ij}(r)$ s obtained from the RMC fits.

and XAFS close to the Ga and Ge K edges and analyzing with the RMC modeling [21]. Owing probably to the above structural information limited to mainly in the first neighboring region, the RMC analysis was performed with large constraints for the first nearest neighbors, i.e., only the Ga-Ga correlations were allowed for the wrong bonds, and their results [21] are also presented in Table II. Nevertheless, the cation-S bond lengths are in good agreement with each other, and the discrepancy is only seen in the Ga-Ga length. As a reference, the results of GaGeSe glass are also given in the table, where the measurements and analyses are performed in the same way except for the lack of the AXS experiment near the S edge. The obtained r_{ij} values are systematically larger due to the larger atomic radius of Se than that of S.

Table II also shows the partial coordination numbers of the first neighbor j th element along the i th element, N_{ij} . The values were calculated from $g_{ij}(r)$ s by integrating up to $r = 0.26$ nm, and the total coordination numbers, N_i , were obtained as the sum around the i th element. Remarkable differences from the previous RMC results by Pethes et al. [21] are found in N_i s. Namely, $N_{\text{Ga}} = 3.55$ largely exceeds the $8 - N$ value of three, although $N_{\text{Ge}} = 3.88$ is near that of four, both of which are smaller than the previous RMC results of 3.85 and 4.07, respectively [21]. It should be noted that $N_{\text{S}} = 2.76$ is much larger than the $8 - N$ value of two and the previous RMC result of 2.13 [21]. Since the $g_{\text{N}}(r)$ result was included in the present RMC calculation, we believe that the obtained N_i results are much more reliable than the previous report [21].

Figure 3 shows three-dimensional (3D) atomic configurations obtained from the present RMC fits, where the small blue, small red, and large yellow balls indicate the Ga, Ge, and S atoms, respectively. In (a) and (b), atomic configurations around the Ga and Ge atoms are marked by drawing polyhedra around them, respectively. At a glance, the polyhedra around the Ga and Ge atoms exhibit individual clusters at the different regions. In (c), the S-S homopolar bonds are represented by orange lines, where the Ga and Ge atoms are made invisible. The S-S bonds also form inhomogeneous configurations. It should be noted that the S-S bond-rich regions are located at the tetrahedra-rich

Table II. r_{ij} and N_{ij} of the GaGeS glass as well as those of the GaGeSe glass. In the case of GaGeSe glass, S in the left column should be replaced with Se.

	r_{ij}				N_{ij}		
	Present 1st	RMC [21]	RMC [8] GaGeSe	Present 2nd	Present	RMC [21]	RMC [8] GaGeSe
Ga-Ga	0.224(1)	0.261	0.280	0.361(2)	0.34	0.29	0.71
Ga-Ge	0.223(1)	–	0.246	0.351(1)	0.54	–	1.32
Ga-S	0.225(1)	0.2275	0.243	0.368(1)	2.67	3.56	1.77
Ga total					3.55	3.85	3.80
Ge-Ga	0.223(1)	–	0.246	0.351(1)	0.36	–	0.76
Ge-Ge	0.222(1)	–	0.236	0.365(2)	0.63	–	1.12
Ge-S	0.222(1)	0.2215	0.236	0.358(2)	2.89	4.07	2.80
Ge total					3.88	4.07	4.68
S-Ga	0.225(1)	0.2275	0.243	0.368(1)	0.59	0.79	0.31
S-Ge	0.222(1)	0.2215	0.236	0.358(2)	0.96	1.36	0.93
S-S	0.218(2)	–	0.236	0.365(1)	1.21	–	1.01
S total					2.76	2.15	2.25

regions around the Ge atoms, i.e., the locations of the Ge tetrahedra and the Se-Se bonds are highly synchronized. These atomic configurations clearly indicate the formation of both the density- and concentration fluctuations in this glass. Note that the same configurations were also observed in the GaGeSe glass [8].

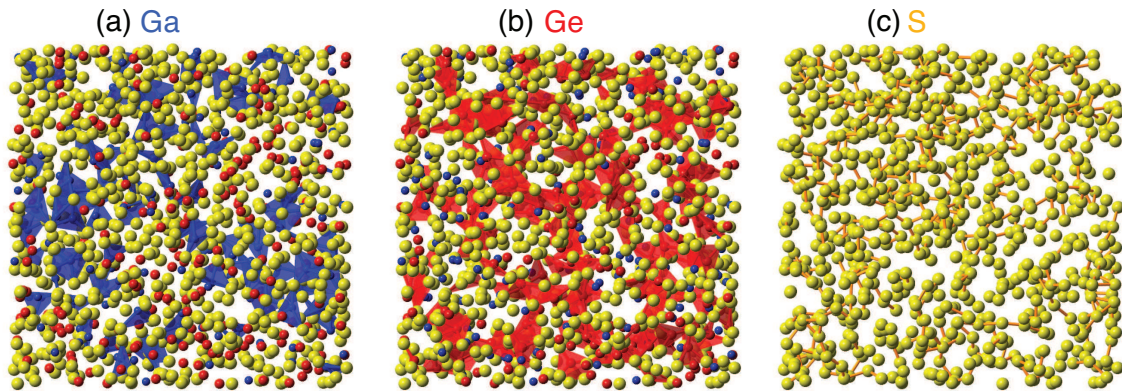


Fig. 3. 3D atomic configurations of Ga, Ge, and S atoms indicated by small blue, small red, and large yellow balls, respectively, obtained from the RMC fits, with polyhedra around the (a) Ga and (b) Ge atoms, and (c) S-S bonds (orange lines).

To be honest, the present analyses are somewhat less than perfect when compared with the previous GaGeSe results [8]. Particularly, the RMC fits to $\Delta_{\text{Ge}}S(Q)$ shown in Fig. 1(a) are insufficient in the first minimum region of about $Q = 20 \text{ nm}^{-1}$, where the fitting quality highly affects the intermediate-range atomic structures around the Ge atoms. As mentioned above, the direct reason for this inconvenience may originate from the lack of $\Delta_{\text{S}}S(Q)$ data in the GaGeS results, which helps the fit quality of the large negative dip in $\Delta_{\text{Ge}}S(Q)$ as seen in Fig. 1 of Ref. [8]. An XAFS experiment close to the S K edge can improve the quality of local atomic arrangements around the S atoms, while it is doubtful for that of the intermediate-range atomic structure because this technique is help-

ful to determine only the nearest-neighbor information. Another method to improve the fits may be to operate the constraints in the RMC modeling procedures. There were no constraints in the current calculation, whereas it would be better to include constraints of coordination numbers if there is additional structural information such as NMR data. Another malfunction is seen again in $\Delta_{\text{Ge}}S(Q)$, where the magnitude of oscillations in the experimental data is much larger than that of the RMC fits. It would come from the overestimate of the theoretical f' value of Ge [12], which may be solved by using experimental data through a detailed measurement of X-ray absorption close to the Ge K edge as was done in Ref. [22].

5. Summary

Local- and intermediate-range atomic structures of $(\text{Ga}_2\text{S}_3)_{0.25}(\text{GeS}_2)_{0.75}$ glass were investigated in detail by the measurements of XRD, AXS close to the Ga and Ge K edges, and ND in combination with RMC modeling. The inclusion of real space $g_N(r)$ data may highly improve the reliability of the coordination number results. The total coordination numbers around the Ga, Ge, and S atoms were determined to be 3.55, 3.88, and 2.76, respectively, which contradict the $8-N$ rule except N_{Ge} and the previous RMC results. Large numbers of wrong bonds of Ga-Ga, Ga-Ge, Ge-Ge, and S-S pairs were observed. Inhomogeneous atomic arrangements were found in both the density and concentration from the obtained 3D atomic configurations, similar to those in the $(\text{Ga}_2\text{Se}_3)_{0.25}(\text{GeSe}_2)_{0.75}$ glass [8].

Acknowledgments

ND measurements were performed at BL21 of the J-PARC MLF (Nos. 2021B0051 and 2017B-0047). AXS experiments were carried out at BL13XU of the SPring-8 (Nos. 2021B1110, 2021A1181, 2019A1556 and 2018B1208). SH acknowledges financial supports by JSPS Grant-in-Aid for Transformative Research Areas (A) ‘Hyper-Ordered Structures Science’ (Nos. 23H04117 and 21H05569) and for Scientific Research (C) (No. 22K12662), and by the Japan Science and Technology Agency (JST) with Core Research for Evolutional Science and Technology (CREST) (No. JPMJCR1861).

References

- [1] B. Bureau, X. H. Zhang, F. Smektala, J.-L. Adam, J. Troles, H.-L. Ma, C. Boussard-Pl  del, J. Lucas, P. Lucas, D. Le Coq, M. R. Riley, and J. H. Simmons, *J. Non-Cryst Solids* **345&346**, 276 (2004).
- [2] J.-L. Adam, L. Calvez, J. Trol  s, and V. Nazabal, *Int. J. Appl. Glass Sci.* **6**, 287 (2015).
- [3] K. Shimakawa, A. Kolobov, and S. R. Elliott, *Adv. Phys.* **44**, 475 (1995).
- [4] V. F. Sears, *Neutron News* **3**, 26 (1992).
- [5] A. W. Mao, B. G. Aitken, R. E. Youngman, D. C. Kaseman, and S. Sen, *J. Phys. Chem. B* **117**, 16594 (2013).
- [6] I. Pethes, R. Chahal, V. Nazabal, C. Prestipino, A. Trapananti, C. Pantalei, B. Beuneu, B. Bureau, and P. J  v  ri, *J. Alloys Compd.* **651**, 578 (2015).
- [7] B. D. Klee, J. R. Stellhorn, M. Krbal, N. Boudet, G. A. Chahine, N. Blanc, W.-C. Pilgrim, T. Wagner, and S. Hosokawa, *Chalc. Lett.* **15**, 1 (2018).
- [8] S. Hosokawa, J. R. Stellhorn, Y. Onodera, S. Kohara, H. Tajiri, E. Magome, L. Pusztai, K. Ikeda, T. Otomo, M. Krbal, and T. Wagner, *JPS Conf. Proc.* **33**, 011069 (2021).
- [9] S. Kohara, K. Ohara, H. Tajiri, C. Song, O. Sakata, T. Usuki, Y. Benino, A. Mizuno, A. Masuno, J. T. Okada, T. Ishikawa, and S. Hosokawa, *Z. Phys. Chem.* **230**, 339 (2016).
- [10] S. Hosokawa, J.-F. B  rar, N. Boudet, W.-C. Pilgrim, L. Pusztai, S. Hiroi, K. Maruyama, S. Kohara, H. Kato, H. E. Fischer, and A. Zeidler, *Phys. Rev. B* **100**, 054204 (2019).
- [11] S. Hosokawa, Y. Wang, J.-F. B  rar, J. Greif, W.-C. Pilgrim, and K. Murase, *Z. Phys. Chem.* **216**, 1219 (2002).
- [12] S. Hosokawa, I. Oh, M. Sakurai, W.-C. Pilgrim, N. Boudet, J.-F. B  rar, and S. Kohara, *Phys. Rev. B* **84**, 014201 (2011).
- [13] S. Sasaki, KEK Report 88-14, (National Laboratory of High Energy Physics, Tsukuba, 1989), P. 1.

- [14] C. H. MacGillavry, and G. D. Rieck (ed.), International Tables for X-ray Crystallography, 2nd ed, (Kynoch, Birmingham, 1968), Vol. III.
- [15] <https://mlfinfo.jp/en/b121/>, (2025).
- [16] S. Hosokawa, Y. Kawakita, L. Pusztai, K. Ikeda, and T. Otomo, J. Phys. Soc. Jpn. **90**, 024601 (2021).
- [17] H. H. Paalman and C. J. Pings, J. Appl. Phys. **33**, 2635 (1962).
- [18] I. A. Blech and B. L. Averbach, Phys. Rev. **137**, A1113 (1965).
- [19] <http://research.kek.jp/group/hydrogen/analysis.html>, (2015).
- [20] O. Gereben, P. J  v  ri, L. Temleitner, and L. Pusztai, J. Optoelectron. Adv. Mater. **9**, 3021 (2007).
- [21] I. Pethes, V. Nazabal, R. Chahal, B. Bureau, I. Kaban, S. Belin, and P. J  v  ri, J. Alloys Compd. **673**, 149 (2016).
- [22] S. Hosokawa, J. R. St  llhorn, N. Boudet, N. Blanc, E. Magome, L. Pusztai, S. Kohara, K. Ikeda, and T. Otomo, J. Phys. Soc. Jpn. **93**, 014601 (2024).